

# MIMO-Based Collision Avoidance in IEEE 802.11e Networks

Abduladhim Ashtaiwi, *Associate Member, IEEE*, and Hossam Hassanein, *Senior Member, IEEE*

**Abstract**—In response to the growing market demand for high-performance wireless local area networks (WLANs) with quality-of-service (QoS) support, the IEEE 802.11 standard adopts the 802.11e as the medium access protocol and 802.11n-based products, which utilize multiple-input–multiple-output (MIMO) transmission systems. The medium access collision avoidance of IEEE 802.11e, even with IEEE 802.11n at the physical layer, still utilizes the enhanced distributed coordination function (EDCF) mechanism. It is known that collisions cause significant performance degradation in IEEE 802.11e EDCF-based systems. In this paper, we utilize the multiple spatial channels of MIMO technology to propose collision-mitigation enhancements to the IEEE 802.11e EDCF. The key idea of the scheme, which is called MIMO-based EDCF (M-EDCF), is the sharing of the spatial channels during the medium contention period, i.e., instead of accessing the medium using all the spatial channels, the accessing nodes use a subset of the available spatial channels. As the number of concurrent spatial channels used is less than or equal to the spatial degree of freedom, receivers can decode the transmitted signals of different medium access contenders and then coordinate their responses to avoid potential collisions. The spatial channel sharing also enables transmitters to sense the medium and terminate if they detect other ongoing medium access attempts. Simulation results show that the M-EDCF scheme substantially reduces medium access collisions. Based on the preliminary results, an adaptive optimized length of the collision-avoidance window is derived. The performance of the M-EDCF scheme based on optimized online spatial channel sharing demonstrates that the scheme further reduces medium access collisions and boosts medium utilization.

**Index Terms**—Medium access control (MAC), performance analysis, protocol capacity, wireless local area network (WLAN).

## I. INTRODUCTION

IEEE 802.11 WiFi networks [1] have become the *de facto* standard for wireless local area networks (WLANs). Future traffic demands require quality-of-service (QoS) provisioning and higher network capacity. To address the former, the IEEE 802.11 Task Group “E” has defined enhancements to the IEEE 802.11 distributed coordination function (DCF) mechanism. The enhancements include defining two main QoS

access functions, i.e., the hybrid coordination function and the enhanced distributed coordination function (EDCF) [2]. To address the latter, the IEEE 802.11n, which utilizes multiple-input–multiple-output (MIMO) transmission systems [3], has been defined.

In this paper, we concentrate on the EDCF access function, which is a contention-based medium access mechanism based on the carrier sense multiple access with collision avoidance. Despite employing a random backoff (BF) prior to each frame transmission attempt and binary exponential BF upon each transmission failure, the most performance-degrading factor of the IEEE 802.11e EDCF protocol is still medium access collisions. We remark though that the EDCF does not make use of the multiple spatial channels made available through IEEE 802.11n. In this paper, we utilize such multiple spatial channels for collision-mitigation enhancements to the IEEE 802.11e EDCF. The key idea of the scheme, which is called MIMO-based EDCF (M-EDCF), is the sharing of the spatial channels during the medium contention period, i.e., instead of accessing the medium using all the spatial channels, the accessing nodes use a subset of the available spatial channels. As the number of concurrent spatial channels used is less than or equal to the spatial degree of freedom, receivers can decode the transmitted signals of different medium access contenders and then coordinate their responses to avoid potential collisions. The spatial channel sharing also enables transmitters to sense the medium and terminate if they detect other ongoing medium access attempts.

In the related literature, there have been numerous studies to improve the performance of the EDCF mechanism. The analytical models proposed in [4] and [5] demonstrated that the performance of the DCF strongly depends on the minimum contention window (CW) and the number of contending nodes. Cali *et al.* [6], [7] proposed a distributed algorithm that enables nodes to estimate the number of contending nodes and then to tune their CW to an optimal value. The work in [8] and [9] proposed schemes in which accessing nodes announce their future BF information in the medium access control (MAC) header of their frame being transmitted. All nodes receiving the information avoid collisions by excluding the same BF duration for their future BF values. The work in [10] identified the relationship between BF parameters, contention level, and channel bit error rate to propose an algorithm that allows a node to dynamically adjust its CW based on the measurement of the channel status. Kim and Hou [11] proposed schemes for modifying the CW size based on the computed network utilization. The latter is then used to determine a

Manuscript received December 10, 2008; revised April 13, 2009 and May 25, 2009. First published June 26, 2009; current version published March 19, 2010. The review of this paper was coordinated by Prof. S. Cui.

A. Ashtaiwi is with the Department of Electrical and Computer Engineering, Queen’s University, Kingston, ON K7L 3N6, Canada (e-mail: 9amaa@queensu.ca).

H. Hassanein is with the School of Computing, Queen’s University, Kingston, ON K7L 3N6, Canada (e-mail: Hossam@cs.queensu.ca).

Color versions of one or more of the figures in this paper are available online at <http://ieeexplore.ieee.org>.

Digital Object Identifier 10.1109/TVT.2009.2026177

scheduling delay that is introduced before a node transmits its pending frame. The work in [12] proposed schemes to avoid collision based on the receiver being the initiator of the communication process. Different proposals of medium access collision-avoidance schemes that are established on exploiting the dual channel mechanisms are presented in [13] and [14]. Fullmer and Garcia-Luna-Aceves [15] proposed the floor-acquisition multiple-access (FAMA) scheme. In FAMA, each ready node has to acquire the medium (the “floor”) before it can use the channel to transmit its data packets. The proposals in [16] and [17] based their collision-avoidance schemes on the power drainage level of the node. The proposed scheme adjusts the CW size according to the accessing node’s power level. Jin *et al.* [18] proposed mitigating the medium access collision in the uplink communication of the infrastructure-based WLANs systems in which all nodes communicate with an access point. The scheme in [18] is based on an oversimplified assumption where nodes are equipped with one transmit antenna and the access point has multiple antennas. However, none of the previously discussed schemes envisions the potential of using the multiple spatial channels of MIMO transmission systems as means to reduce medium access collisions in IEEE 802.11 EDCF-based systems.

In this paper, we introduce a novel M-EDCF. M-EDCF is the first such protocol that exploits MIMO properties to enhance the IEEE 802.11e EDCF collision-avoidance mechanism. The basic idea is the sharing of the multiple spatial channels of MIMO technology during medium contention periods to mitigate medium access collisions. Simply, instead of accessing the medium using all the spatial channels, the contending nodes only use a subset of the available spatial channels. As the concurrent spatial channels used are less than or equal to the spatial degree of freedom, the receivers can still decode the multiple transmitted signals. The proposed spatial-channel-sharing scheme enables other collision-avoidance mechanisms, such as medium contention termination and medium contention selection (MCS). The former refers to the capability of terminating the ongoing medium access attempt if the accessing node detects other medium access attempts. MCS refers to the ability to detect multiple concurrent medium access signals transmitted by different medium access contenders. This new capability enables receivers to implement response coordination schemes. Both the medium contention termination and selection can further be exploited to reduce the IEEE 802.11e EDCF collision rate and incorporate QoS-differentiation schemes. In addition, optimal spatial channel sharing (i.e., the number of spatial channels exploited by each contending node) is proposed. The optimal spatial-channel-sharing scheme is based on the estimation of the number of active nodes and then the finding of the optimal spatial channel value that maximizes the system performance in terms of reducing the medium access collision and increasing the transmission medium utilization.

Simulation results obtained using the OPNET Modeler show that incorporating the M-EDCF scheme considerably reduces the medium access collisions and boosts the transmission medium utilizations. The optimal spatial-channel-sharing scheme is also evaluated. The results obtained demonstrate that,

with different traffic loads, the use of the adaptive spatial channel sharing consistently outperforms that of the fixed spatial channel sharing.

The remainder of this paper is organized as follows: In Section II, we present some background material. Section III explains how the MIMO multiple spatial channels can be exploited to enhance the IEEE 802.11e EDCF collision-avoidance mechanism. In Section IV, we present simulation results of the M-EDCF scheme over a single-hop network. Section V details the optimal spatial-channel-sharing scheme. In Section VI, we evaluate the M-EDCF scheme over a multihop network. Concluding remarks are given in Section VII.

## II. IEEE 802.11-BASED WLANs

The IEEE 802.11 DCF priority access to the transmission medium is controlled through the use of interframe space (IFS) time intervals between the transmission of frames. The IEEE 802.11 standard specifies three different IFS time intervals, ranging from shortest to largest: 1) short IFS (SIFS); 2) point coordination function IFS (PIFS); and 3) DCF IFS (DIFS). To ensure that multiple stations do not transmit at the same time, after the DIFS period, the DCF medium access function performs a BF that is randomly selected, using the uniform distribution function, from the CW range. Once the BF timer counter reaches zero, the node is authorized to access the transmission medium. To support QoS differentiation, Task Group “E” (IEEE 802.11e [2]) extends the IEEE 802.11 MAC protocol by defining four different access classes (ACs). Access to the transmission medium is then granted based on the priorities of data traffic such that each AC first waits for a differentiated arbitration IFS (AIFS[AC]) and then performs a differentiated BF.

To improve the WLAN throughput, the IEEE 802.11 Task Group “N” (TGn), i.e., IEEE 802.11n, builds on the existing IEEE 802.11 standards by adding multiple transmit and receive antennas (called MIMO transmission system) to create multiple spatial channels that are capable of simultaneous receive or transmit traffic [3]. To help receivers estimate the spatial channel status and therefore recover the transmitted signals, the IEEE 802.11n amendment recommends transmitting a known communication setup frame called sounding frames (SFs) through all transmit antennas. As defined in the IEEE 802.11n amendment, the SFs can be either attached to the MAC protocol data unit frames if no spatial channel feedback information is required at the transmitter node or through two-way handshake exchanges. In the latter case, the transmitter sends a Channel Sounding reQuest (CSQ), and the receiver responds with a channel sounding response (CSR). The CSQ and CSR exchange is performed when the spatial channel feedback information is required at both sides, i.e., the transmitter and receiver nodes. During the CSQ period, the transmitter node concurrently sends one SF through each transmit antenna element. Then, the receiver, after receiving the CSQ frames, responds by concurrently sending one SF through each transmit antenna element of the receiver node, where the latter is done during the CSR period. In this work, we consider the two-way-handshake SF exchange.

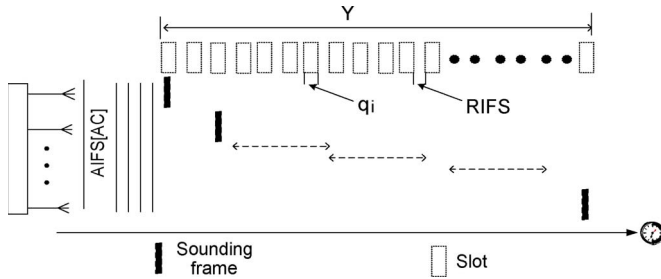


Fig. 1. SF transmission window.

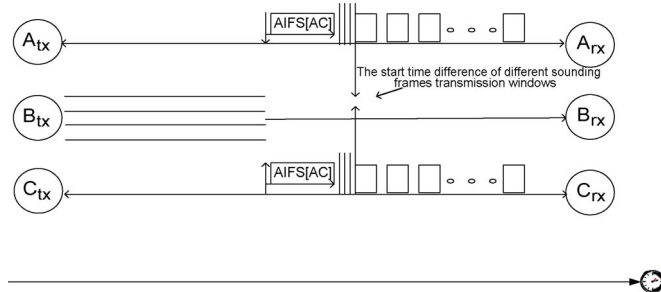


Fig. 2. Synchronization of the SF transmission windows.

### III. MIMO-BASED ENHANCEMENTS TO THE IEEE 802.11e EDCF COLLISION-AVOIDANCE MECHANISM

In this work, we consider a multihop environment (viz., ad hoc networks) where each node is equipped with  $n_t$  transmit and  $n_r$  receive antennas. Let  $an_i^{tx}$ ,  $\{i = 1, 2, \dots, n_t\}$  and  $an_i^{rx}$ ,  $\{i = 1, 2, \dots, n_r\}$  represent the  $an_i^{tx}$  transmit and  $an_i^{rx}$  receive antenna elements, respectively. At any node in the network, the network is viewed at this node [node in question (NiQ)] and its neighbors, i.e., nodes whose transmission ranges overlap with the NiQ. Upon reaching zero BF countdown, instead of accessing the transmission medium by sending a request-to-send (RTS) or data frame, to avoid collision, the accessing node starts with sending an SF over each of its transmit antenna elements. Let  $\gamma = \{1, 2, \dots\}$  denote the SF transmission window, which consists of slot(s) during which the accessing node transmits all its SFs, as shown in Fig. 1. Let  $q_i$ ,  $i = \{1, 2, \dots, \gamma\}$  represent the  $i$ th slot at which  $an_i^{tx}$  transmits its SF. Reduced IFS is an idle time interval (in seconds) that the IEEE 802.11n uses to separate sequential SF transmissions, as shown in Fig. 1. On the one hand, the accessing node may concurrently send its SFs during the same slot  $i$ , i.e.,  $\gamma = 1$ . This method is implemented by the IEEE 802.11n MAC protocol. Hence, throughout this work, when  $\gamma = 1$ , we refer to the IEEE 802.11n amendment. On the other hand, the accessing node may send its SFs over multiple slots, i.e.,  $\gamma > 1$ .

Nodes in ad hoc networks synchronize the start of their SF transmission windows using common IFS intervals to the transmission medium status changes, which they all sense. To explain this, let us consider the example shown in Fig. 2, where we have three connection pairs:  $A(t_x, r_x)$ ,  $B(t_x, r_x)$ , and  $C(t_x, r_x)$  in the same contention area. Initially, connection pair  $B(t_x, r_x)$  is communicating, whereas connections  $A(t_x, r_x)$  and  $C(t_x, r_x)$  are deferring for  $B(t_x, r_x)$ . At the end of the

connection  $B(t_x, r_x)$  transmission, connections  $A(t_x, r_x)$  and  $C(t_x, r_x)$  sense the medium to be changed; hence, they start contending for the medium, and the procedure starts by first waiting for an IFS time to elapse and then performing BF countdown. In single-hop networks, there are two possible outcomes: The first case is where both connections  $A(t_x, r_x)$  and  $C(t_x, r_x)$  select the same BF number and reach their zero countdown at the same time. In this case, the start times of the SF transmission windows of both connections are the same. Accordingly, the receivers receive aligned frames. The other case happens when either connection  $A(t_x, r_x)$  or connection  $C(t_x, r_x)$  reaches its zero countdown earlier than the other connection. Since this is a distributed medium access procedure, the time they reach zero could be different. On the one hand, if the medium access difference between the two connections is shorter than or equal to the propagation delay, then both connections begin with their SF transmission windows misaligned. On the other hand, if the medium access difference between the two connections is greater than the propagation delay, only one connection proceeds, whereas the other defers, because it notices the start transmission of the first connection.

Longer  $\gamma$  lengths enable the contending nodes to share the spatial channels of MIMO during the medium access period. Hence, even with multiple concurrent transmissions (by different transmit nodes), receivers can still decode the multiple transmitted signals as long as the number of transmitted SFs is less than or equal to the spatial degree of freedom  $\varphi$ . Hence, the core of our proposed scheme for enhancing the IEEE 802.11 EDCF collision-avoidance mechanism is based on varying the  $\gamma$  length to avoid having more than  $\varphi$  signals transmitted during the same time slot. By varying the value of  $\gamma$ , the contending nodes can perform two actions.

- 1) Early medium contention termination (EMCT): If the contending nodes use longer  $\gamma$  lengths such that they can switch to the listening mode during idle slots, the contending nodes can sense the transmission medium activity while they are currently contending. This capability enables the accessing nodes to implement early collision resolution where they terminate their medium access earlier if they detect other ongoing medium access attempts. In addition to collision avoidance, the accessing nodes may terminate their medium access in accordance with any system performance metric requirements, such as supporting QoS (where only lower priority nodes are required to terminate); being collision-avoidance conservative (considering longer  $\gamma$  lengths, which make nodes more attentive to other node medium access contentions); and/or saving bandwidth (terminate medium access attempts that have higher probability of ending up with a collision). Node C in Fig. 3(a) performed early termination, because it had detected another medium access attempt by node B. This is compared with Fig. 3(b), where  $\gamma = 1$  and node C does not detect the other medium access attempt, hence causing a collision with the data received at node B. Algorithm 1 summarizes the procedure followed by the transmitter during the contention period. The collision-avoidance procedure, as presented by the

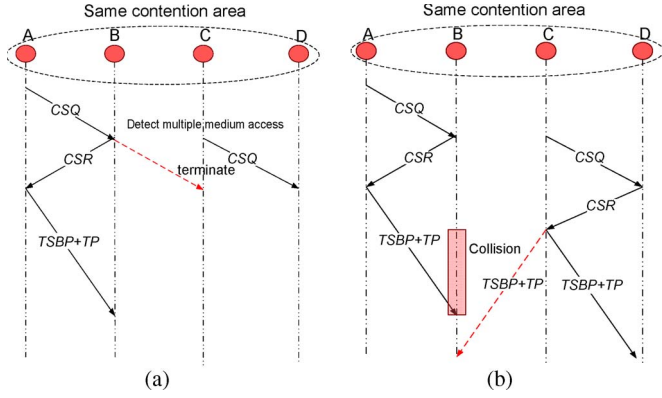


Fig. 3. Medium contention at the transmitters. (a) Multiple medium contentions when  $\gamma > 1$ . (b) Multiple medium contentions when  $\gamma = 1$ .

code of Algorithm 1, starts when the BF countdown of an access node reaches zero (line 1). It first determines its  $\gamma$  length and then uses the uniform distribution function to find  $q_i$  for each transmit antenna element (lines 2–6). The slots  $(q_i, 1, 2, \dots, n_t)$  are then stored in chronological order (line 7). Medium access termination is performed if the EMCT procedure is required and possible (lines 8–14). Alternatively, it sends the SFs over its antenna at their selected slots (line 16).

- 2) MCS: Adopting longer  $\gamma$  lengths can help receivers detect multiple medium access contenders (signals). This capability enables receivers to implement response coordination such as responding to a particular AC to enhance QoS differentiation or keeping silent if the node's response may cause a collision with other nodes. Fig. 4(a) shows the scheme when the accessing nodes adapt a longer  $\gamma$  length. Node C receives CSQ from D and CSR from B, and C does not respond to node D, as its response can cause a collision with B. The same scenario is repeated for  $\gamma = 1$ , i.e., the access nodes concurrently send the SFs over their antennas. As shown in Fig. 4(b), the total number of spatial streams from B and D exceeds  $\varphi$ ; therefore, C cannot decode the received signal. Node C responds to the next CSQ request from D, which causes a collision with the data received at B. Algorithm 2 lists the procedure followed by the receiver during the contention period.

**Algorithm 1** M-EDCF transmitter medium access procedure

- 1: **if**  $BF \leftarrow 0$  **then**
- 2:   *determine*( $\gamma$ )
- 3:   **for**  $an_i^{tx} \forall_i, i = 1, 2, \dots, n_t$  **do**
- 4:      $q_i \leftarrow \text{uniform}(0, \gamma)$
- 5:      $i++$
- 6:   **end for**
- 7:   *sort*( $q_i$ )
- 8:   **if** EMCT  $\leftarrow TRUE$  **then**
- 9:     **if**  $IDL > \Delta$  **then**
- 10:       Switch to listening mode, and sense the transmission medium.
- 11:       **if** the NiQ detects other medium access attempts **then**

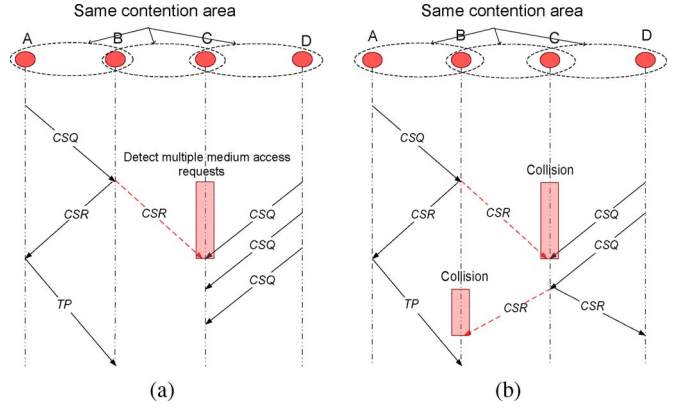


Fig. 4. Medium contention at the receivers. (a) Multiple medium contentions when  $\gamma > 1$ . (b) Multiple medium contentions when  $\gamma = 1$ .

- 12:       Terminate the medium access attempt.
- 13:     **end if**
- 14:   **end if**
- 15:   **else**
- 16:     Send the SFs at their specified slots without switching to listening mode.
- 17:   **end if**
- 18: **end if**

*IDL*: time interval between consecutive SF transmissions.

$\Delta$ : time interval that is sufficient for switching and listening to the transmission medium.

**Algorithm 2**: M-EDCF receiver medium access procedure

- 1: **if** a single CSQ request is received **then**
- 2:   Respond with CSR after SIFS time.
- 3: **else if** multiple CSQ requests are destined to this node **then**
- 4:   Respond with CSR to the first finished CSQ node.
- 5: **else if** multiple CSQ and CSR requests are received **then**
- 6:   Do not respond.
- 7: **end if**

#### IV. PRELIMINARY RESULTS

In this section, we perform a preliminary evaluation of the M-EDCF scheme. We first detail the simulation model and then present the simulation results, which are compared with those of the IEEE 802.11n MAC protocol.

##### A. Simulation Model

Utilizing OPNET modules, we have modified the built-in IEEE 802.11e physical and MAC layers to include all the details of the M-EDCF scheme. Seven modifications are given here.

- 1) We add multiple transmit-and-receive antenna elements. Each transmit and receive antenna element is modeled using the built-in wireless transmit-and-receive module of the OPNET Modeler, respectively. Similar to the IEEE 802.11n draft [3], we consider  $n_t = n_r = 4$ .
- 2) We modify the interaction between the physical and MAC layers to accommodate the increased number of

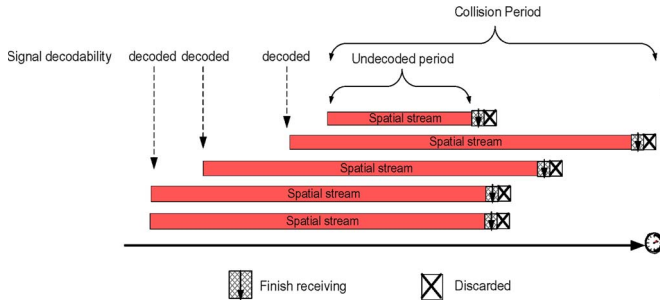


Fig. 5. Instantaneous signal decode ability with  $\varphi = 4$ .

TABLE I  
IEEE 802.11n PARAMETER SETTINGS

parameter	value	parameter	value
$CW_{min}$	15	$CW_{max}$	1023
SIFS	$16 \mu s$	PMDU	500-65535 byte
RIFS	$2 \mu s$	q	$30 \mu s$

transmit-and-receive antenna elements, such as performing spatial stream multiplexing and demultiplexing.

- 3) We insert the SF transmission phase before sending RTS frames, which include exchanging the SFs through all transmit antenna elements.
- 4) We build the packet structure of the SF using the packet module of OPNET.
- 5) We consider a Rayleigh slow-fading channel with a very rich scattering environment and that the transmit and receiver antennas are spaced sufficiently apart such that the channel gain matrix is independent identically distributed. We assume that  $\varphi$  is equal to  $\min(n_r, n_t)$  [19], [20]. Based on the defined degree of freedom, Fig. 5 shows the instantaneous signal decode-ability model that we used in this work. To explain the figure, consider a receiver equipped with four receiving antennas. In addition, consider five transmitting nodes, with each node equipped with one transmitting antenna. We consider that the receiver can receive and decode all the incoming spatial streams as long as the number of spatial streams is less than or equal to the number of receiving antennas, which is equal to  $n_r$  in our model. If these transmitters start transmitting their streams, the instantaneous signal decode ability at the receiver is modeled as shown in Fig. 5. Spatial streams that experience any collision period are discarded at the end. We also consider that, if a collision occurs, the collision period lasts as long as the received signal has an overlapping portion with the collided signals.
- 6) Since IEEE 802.11n is not yet modeled by the OPNET Modeler, we have also modified the IEEE 802.11e module to include the defined IEEE 802.11n physical and MAC enhancements. This includes adding multiple transmit-and-receive antennas that are attached to the multiplexing and demultiplexing modules.
- 7) The parameters for the physical and MAC layers used for both models follow those defined for the IEEE 802.11n amendment and are summarized in Table I.

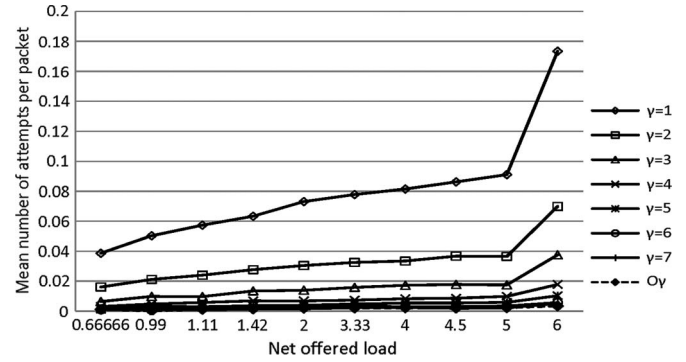


Fig. 6. Mean number of attempts per packet for different  $\gamma$  lengths and network loads.

The nodes are configured to generate traffic that follows a Poisson distribution with a mean arrival that is equal to  $\lambda$ . For each generated data packet, the nodes select a random neighbor as the final destination for this packet. During the simulation, we change the following parameters:

- 1)  $\lambda$ : simulation parameter that assumes different values to model the network loads;
- 2)  $\gamma$ : SF transmission window length during which an accessing node must transmit an SF over each of its transmit antenna elements.

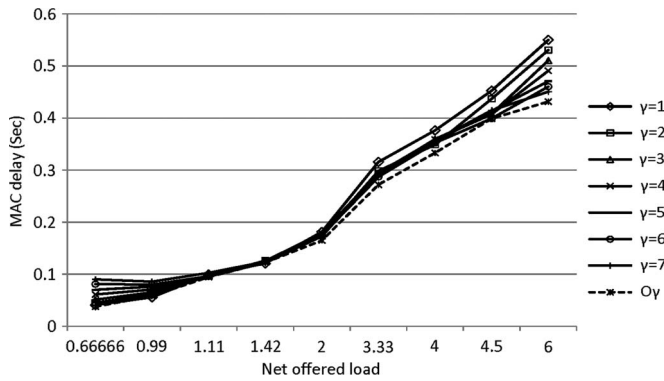
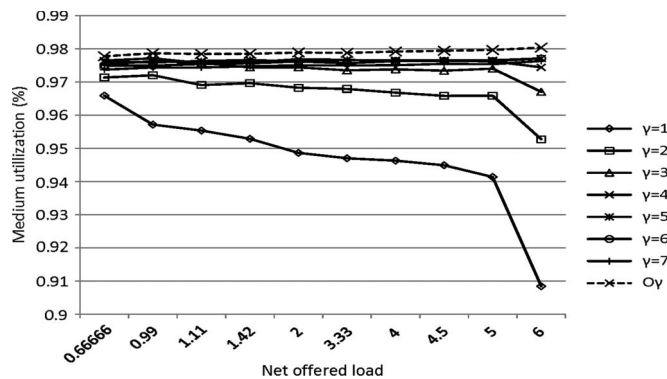
### B. Performance Metrics

We observe four performance metrics.

- 1) average throughput: the total number of successfully delivered bits divided by the lifetime of the simulation;
- 2) mean number of attempts per packet: the average number of transmission attempts per successfully delivered packet;
- 3) average MAC delay: the time from inserting the packet in the queue until it starts transmission. The MAC delay is composed of two delay components, i.e., the BF delay and the incorporated M-EDCF scheme delay, which is the time spent in the exchange of CSQ and CSR;
- 4) medium utilization: defined as  $U = (T_d / (T_c + T_d))$ , where  $T_d$  is the time spent in transmitting successful data, and  $T_c$  is the total control time, which includes all the time spent in exchanging the coordination messages until a successful transmission.

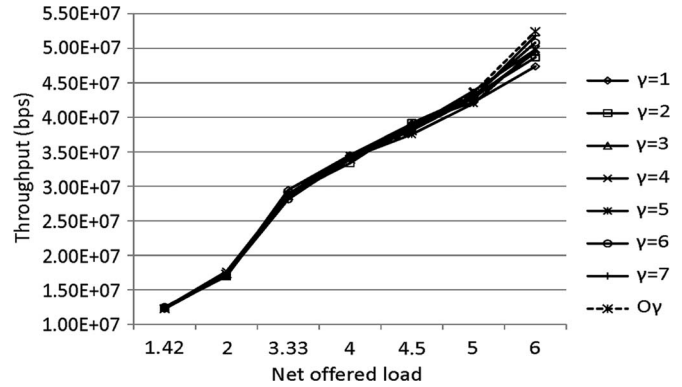
### C. Simulation Results: Single-Hop Network

The single-hop case is configured with 16 nodes that are distributed in the transmission range of each other using a uniform distribution function. In all the experiments, 90% confidence levels are maintained with 10% confidence intervals based on ten independent runs. Fig. 6 shows the mean number of attempts for different  $\gamma$  lengths and network loads. As expected, the number of collisions for smaller  $\gamma$  lengths tends to rapidly increase as the network traffic load increases. This is because smaller  $\gamma$  lengths cause the accessing nodes to send their SFs over shorter  $\gamma$  lengths, which make the total number of transmitted spatial streams exceed  $\varphi$ . Fig. 7 shows the MAC

Fig. 7. MAC delay for different  $\gamma$  lengths and network loads.Fig. 8. Channel utilization for different  $\gamma$  lengths and network loads.

delay. Because collisions are rare in lightly loaded networks, the MAC delay is dominated by the M-EDCF scheme delay. This is shown in Fig. 7, where the scheme's performance under smaller  $\gamma$  lengths has lower MAC delay, compared with that under longer  $\gamma$  lengths. As the network load increases, the number of collisions also increases; therefore, the MAC delay is dominated by the BF delay as collided packets have to wait for longer BF time, and sometimes, the same packet experiences multiple collisions before being successfully transmitted, which means increasingly longer BF delays.

Next, we study the impact of implementing the M-EDCF scheme on medium utilization. Fig. 8 shows the system utilization at different values of  $\gamma$  lengths and network loads. The performance gap between longer and shorter  $\gamma$  lengths increases as the network load increases. (Longer  $\gamma$  lengths result in better performance.) This is because collisions have higher negative impact on the medium utilization. Fig. 9 shows the effect of changing the  $\gamma$  length and the network loads on the throughput. Under a light network load, all the arriving traffic are delivered before the end of the simulation time. This is because, even with collisions resulting from the use of shorter  $\gamma$  lengths, there is still enough time to retransmit and deliver the collided packets. This explains the alignment of curves, at a light network load, of all used  $\gamma$  lengths. As the network load increases (with a higher traffic rate of 5 packet/node/s), the performance under longer  $\gamma$  tends to perform better than that under shorter lengths. The higher performance gap, in the throughput, of longer  $\gamma$  is due to the fact that longer  $\gamma$  lengths avoid more collisions, which save some bandwidth to deliver

Fig. 9. Throughput for different  $\gamma$  lengths and network loads.

more data. Hence, under a high network load, the performance of longer  $\gamma$  lengths has a higher average throughput than that with shorter  $\gamma$  lengths.

As stated previously, the M-EDCF scheme activates two modes of operations, i.e., EMCT and MCS. Fig. 10(a) shows the difference in the number of attempts per packet between activating and silencing both modes EMCT and MCS. Activating both modes can further avoid collisions, compared with silencing both modes. Longer  $\gamma$  lengths allow the nodes to detect more medium access attempts; hence, the nodes can perform more terminations, which can result in a lesser number of collisions, compared with those with smaller  $\gamma$  lengths. Fig. 10(b) shows the difference in the MAC delay between activating and silencing both modes. The combination of having fewer collisions (i.e., by activating the EMCT mode) and first selecting the CSQ requests (i.e., by activating the MCS mode) results in smaller MAC delay, compared with silencing both modes.

## V. OPTIMAL SPATIAL CHANNEL SHARING

Earlier results show the system performance for different  $\gamma$  lengths and network loads. It is clear that, even with a slightly loaded network, adapting a longer  $\gamma$  can prevent a very considerable amount of collisions, compared with adapting a smaller  $\gamma$  length. We can also observe that longer  $\gamma$  lengths at light network loads tend to have slightly higher MAC delays. In this section, we first observe the effect of changing the  $\gamma$  length on the system performance, and then, we formulate an optimization program that finds the optimal value of  $\gamma$  that maximizes the system performance in terms of collision avoidance and transmission medium utilization.

### A. Effect of $\gamma$ Length

Fig. 11 shows the effects of changing the  $\gamma$  length on the transmission medium utilization and on the MAC delay for two sample values of randomly selected arrival rates, i.e., 1 and 1.5 packet/node/s. Fig. 11(a) and (c) shows the MAC delay for different values of  $\gamma$  lengths. Changing the  $\gamma$  length produces MAC delay values with concave-up curve shape where the MAC delay first starts at higher values, then drops, and, finally, increases again. Accordingly, changing the  $\gamma$  lengths has a concave-down-curve effect on the medium

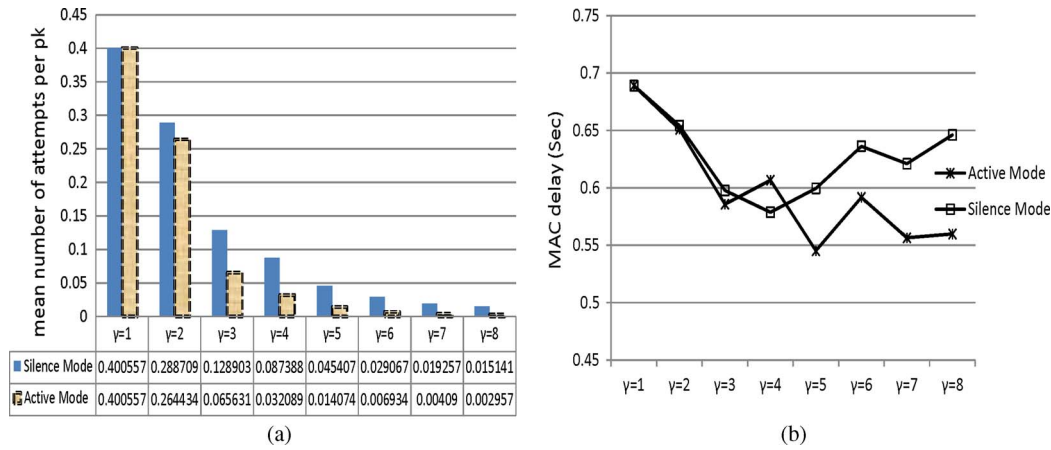


Fig. 10. Activation versus silencing of EMCT and MCS collision-avoidance enhancement mechanisms. (a) Mean number of attempts per packet difference between active and silence EMCT MCS modes. (b) MAC delay difference between active and silence EMCT MCS modes.

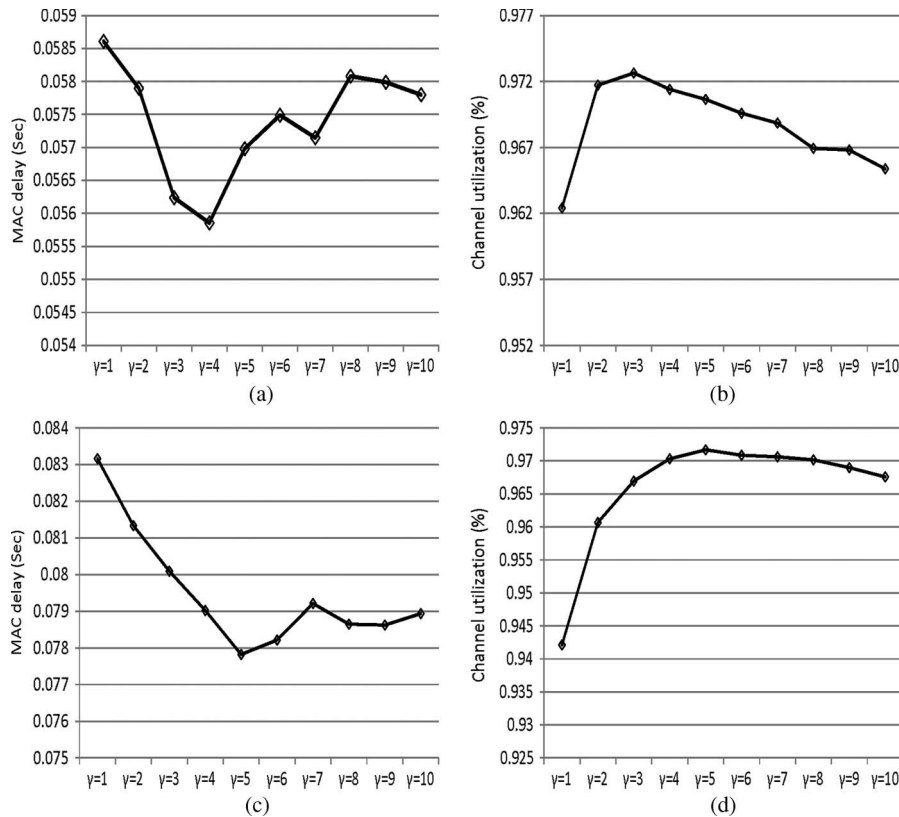


Fig. 11. Effect of changing  $\gamma$ . (a) Effect of changing the  $\gamma$  length on the MAC delay when the traffic load is equal to 1 packet/node/s. (b) Effect of changing the  $\gamma$  length on the channel utilization when the traffic load is equal to 1 packet/node/s. (c) Effect of changing the  $\gamma$  length on the MAC delay when the traffic load is equal to 1.5 packet/node/s. (d) Effect of changing the  $\gamma$  length on the channel utilization when the traffic load is equal to 1.5 packet/node/s.

utilization, as shown in Fig. 11(b) and (d). By observing the overall system performance in Fig. 11, we notice that the best system performance of different traffic loads (1 and 1.5 packet/node/s) happens at different  $\gamma$  length values per traffic load. For example, the maximum medium utilization and the minimum MAC delay for the traffic load of 1 packet/node/s are achieved when  $\gamma = 3$ , whereas  $\gamma = 5$  achieves the best system performance when the traffic load is equal to 1.5 packet/node/s. According to our extensive offline simulation, we observed that the concave-up and concave-down curves are formed for all values of the arrival rate. The minimum and maximum observed

results occur at different values of  $\gamma$ , depending on the system parameters.

### B. Optimal $\gamma$ Length

Based on the observation in the previous section, we propose an online scheme by which each contending node, during the runtime and according to the variations of the traffic load, adapts its  $\gamma$  to an optimal  $\sigma\gamma$  length so that the selected length avoids collisions and maximizes the medium utilization. Our proposed  $\gamma$  adaptability scheme is considered in single-hop

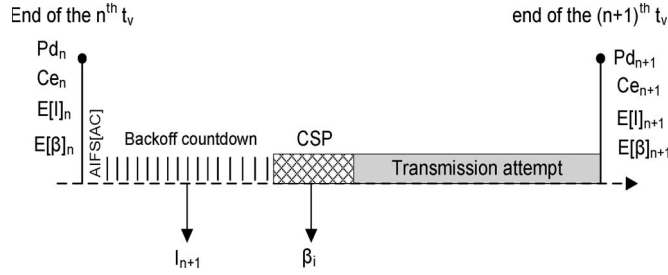


Fig. 12. Virtual transmission period.

networks, where all nodes hear the same medium. The proposed scheme is based on sensing the transmission medium activity to estimate the number of active antenna  $v$ , where  $v = C_e \times n_t$ .  $C_e$  is the number of active nodes (those with data packet(s) ready for transmission).  $C_e$  is estimated by monitoring the transmission medium activity using carrier sensing during the virtual transmission  $t_v$  interval. The latter, as shown in Fig. 12, is the span of time between the observation of the AIFS[AC] period and the end of a transmission attempt, i.e., the successful or collided transmission attempt.  $C_e$  estimation is based on counting the number of consecutive idle slots  $I$  in each virtual transmission period. This value is then substituted in an exponential moving average function to compute the average  $E[I]$  given by

$$E[I]_{n+1} = \alpha \times E[I]_n + (1 - \alpha) \times I_{n+1} \quad (1)$$

where  $\alpha$  is the smoothing factor. As discussed in [6],  $E[I]_{n+1}$  and the current transmission probability  $Pd_{n+1}$  can be used to estimate the number of active nodes

$$C_{\text{comp}} = \frac{\ln\left(\frac{E[I]_{n+1}}{E[I]_{n+1} + T_{\text{slot}}}\right)}{\ln(1 - Pd_{n+1})} \quad (2)$$

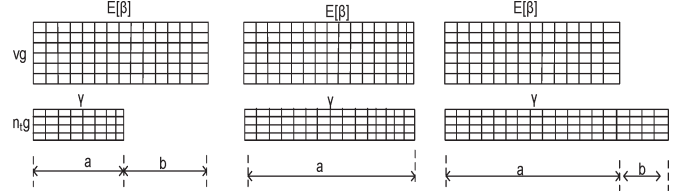
where  $T_{\text{slot}}$  is the MAC-layer slot time. The computed active node  $C_{\text{comp}}$  is then substituted in the exponential moving average function to smooth the variations that result from the network traffic load fluctuations as follows:

$$C_{e_{n+1}} = \alpha \times C_{e_n} + (1 - \alpha) \times C_{\text{comp}}. \quad (3)$$

$Pd_{n+1}$  in (2) expresses the probability that a node transmits in a randomly chosen slot  $T_{\text{slot}}$  [6]. Given  $E[I]_{n+1}$ ,  $Pd_{n+1}$  can be approximated as  $Pd_{n+1} = (1/(2 \times E[I]_n))$  [21].

Hereinafter, we differentiate between two types of SF transmission windows, i.e.,  $\gamma$  and  $E[\beta]$ . The former is the SF transmission window adapted by the NiQ to transmit its SFs.  $E[\beta]$  is the average SF transmission window length considered by the  $C_e$  nodes during the previous virtual transmissions. The  $E[\beta]$  computation is performed by observing the medium activity during each  $t_v$  period and recording the lengths of the SF transmission windows  $\beta_i$ ,  $i = \{1, 2, \dots, C_e\}$  adapted by the contending nodes (neighbors) to transmit their SFs. During each virtual transmission and at the end of each SF transmission of each contending node, the NiQ observes the  $\beta_i$  length and computes the average  $E[\beta]_{n+1}$  given by

$$E[\beta]_{n+1} = \alpha \times E[\beta]_n + (1 - \alpha) \times \beta_{i_{n+1}}. \quad (4)$$


 Fig. 13.  $\gamma$  variability.

Let  $m = 1, 2, \dots, (v + n_t)$  represent the number of contending antennas that may transmit an SF in the generic slot  $q_i$ . At any contending node,  $m$  consists of two groups of contending antennas, i.e., the NiQ's antennas group  $n_tg$  and the antenna group of the  $C_e$  contending nodes  $vg$ . Let  $p(m)$  be the probability that  $m$  antennas transmit in a generic slot  $q_i$ .  $p(m)$  is a function of the number of contending antennas of each contending group (i.e.,  $n_tg$  and  $vg$ ) and their transmission probabilities (i.e.,  $1/\gamma$  and  $1/E[\beta]$ ), respectively. According to MIMO properties, receivers can decode signals if the number of streams (transmitting antennas) is less than or equal to  $\varphi$ . Allowing more than  $\varphi$  antennas to transmit in a slot causes collision and hence must be avoided. Accordingly, we denote  $p_s(0 < m \leq \varphi)$  as the probability of success. Based on the knowledge of  $vg$ ,  $1/E[\beta]$ , and  $\varphi$ , the NiQ can adapt its transmission probability by varying its  $\gamma$  length to maximize the success probability, i.e., permitting any number (between one and  $\varphi$ ) of antennas only to transmit. Fig. 13 shows how the NiQ can vary its SF transmission window to increase the probability of having the desired number of allowed transmitting antennas. Fig. 13 also shows that varying the  $\gamma$  window length results in three cases i.e.,  $\gamma < E[\beta]$ ,  $\gamma = E[\beta]$ , and  $\gamma > E[\beta]$ . Let  $\tau$  represent the number of slots. By letting  $\tau = \max(\gamma, E[\beta])$  (see Fig. 13),  $\tau$  can be divided into two subsets of slots, i.e., slot sets  $a$  and  $b$ . The  $p_s(0 < m \leq \varphi)$  of the former slots are affected by the transmission probability of both contending antenna groups  $n_tg$  and  $vg$ . The latter slots are only affected by one or the other contending antenna group, i.e., either  $n_tg$  or  $vg$ , depending on whichever is longer. Since the slots of set  $a$  are the slots impacted by both contending groups (i.e.,  $n_tg$  and  $vg$ ), we can only study the collision probability in these slots.

Let the combinations of the transmission number of  $n_tg$  and  $vg$  at a generic slot  $q_i$  of slot set  $a$  represent the sample space. Let the number of transmit antenna combinations within this range  $0 < m \leq \varphi$  represent the success event. Therefore, the success outcome events can formally be defined as

$$p_s(0 < m \leq \varphi) = \left(1 - \frac{1}{w_i \times \gamma}\right)^{n_t} \sum_{r=1}^{\varphi} \binom{v}{r} \left(\frac{1}{E[\beta]_n}\right)^r \left(1 - \frac{1}{E[\beta]_n}\right)^{v-r} + \sum_{j=1}^{n_t} \left(\binom{n_t}{j} \left(\frac{1}{w_i \times \gamma}\right)^j \left(1 - \frac{1}{w_i \times \gamma}\right)^{n_t-j} \times \sum_{r=0}^{n_t-j} \binom{v}{r} \left(\frac{1}{E[\beta]_n}\right)^r \left(1 - \frac{1}{E[\beta]_n}\right)^{v-r}\right). \quad (5)$$

Equation (5) breaks down the transmission antennas into two transmission groups, i.e., the NiQ and  $C_e$  antenna groups. A successful transmission on a transmission medium only

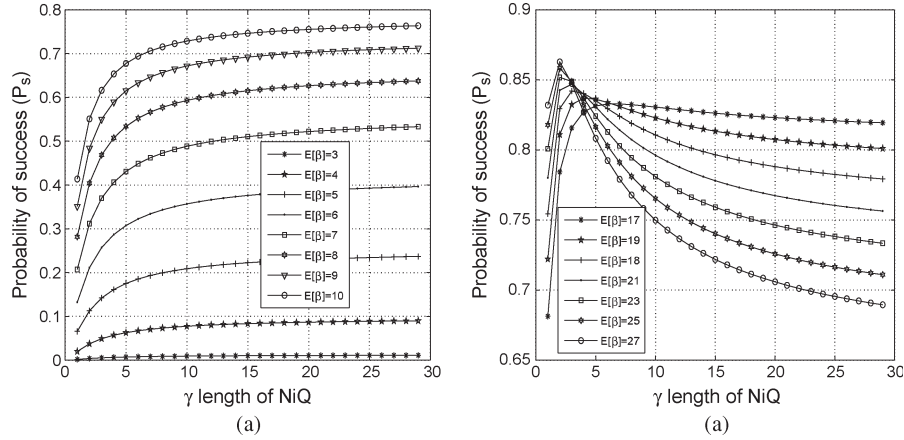


Fig. 14. Success probability as a function of different values of  $\gamma$  and  $\beta$ . (a) Case when  $vg$  and/or their transmission probability is high. (b) Case when  $vg$  and/or their transmission probability is low.

happens if the number of used antennas (regardless of how many nodes use how many antenna) is less than or equal to  $\varphi$ . In the first term, (5) satisfies the preceding statement by computing the probability that none of the NiQ antennas will transmit multiplied by the probability that one to  $\varphi$  antenna of  $v$  antennas will transmit. The result is then added to the second term, which computes the probability that  $j = 1, 2, \dots, n_t$  antennas of the NiQ will transmit multiplied by the probability that  $n_t - j$  antennas of the  $v$  antennas will transmit.  $w_i$  is the weight of a class  $i$ , which is introduced to modify the transmission probability considered by different contending nodes to enable medium access differentiation among different ACs. The higher the AC, the lower the assigned weight factor. Assigning smaller weight factors to  $w_i$  permits the contending nodes of higher priority traffic to finish the transmission of their SFs earlier; hence, they can be selected by the respective receivers before those nodes with higher weight factor. However, assigning larger weight factors to  $w_i$  causes nodes with lower priority traffic to use longer  $\gamma$  lengths, which have the following advantages: 1) Nodes with longer  $\gamma$  lengths have more idle slots, where they can listen to the medium activity, which makes them more attentive to other transmissions (e.g., transmission of higher priority traffics). 2) Longer  $\gamma$  lengths permit other nodes, which use shorter  $\gamma$  lengths, to get selected first. Generally, modifying the transmission probability of nodes by changing their assigned weight factors can be adapted to achieve different desirable performance metrics, such as QoS prioritization, early collision resolution, and being more conservative.

Using (5), Fig. 14 shows the success probability for different values of  $\gamma$  and  $E[\beta]$  for  $vg = 18$  and  $n_t g = 4$ . As shown in Fig. 14, the success probability depends on the value of the transmission probability of the NiQ's neighbors. If the transmission probability of the NiQ's neighbors is high, increasing the transmission probability of the NiQ reduces the success probability. Conversely, if the transmission probability of the NiQ's neighbors is low, increasing the transmission probability of the NiQ increases the success probability. Hence, the probability of success can be divided into two cases: The first case (Case 1) occurs when the transmission probability of the  $vg$  antennas is high (i.e., when  $E[\beta]$  is small); in this case, maximizing the success probability requires the NiQ to

consider very low transmission probability, i.e., using longer  $\gamma$  lengths. The second case (Case 2) occurs when the transmission probability of the  $vg$  antennas is low (i.e., when  $E[\beta]$  is high); in this case, the maximum success probability is achieved by considering high transmission probability by the NiQ, i.e., shorter  $\gamma$  lengths. Based on this observation, we formulate an optimization program that is independently used by the NiQ to find the  $\sigma\gamma$  length. The optimization problem is formulated as follows:

$$\max(p_s(0 < m \leq \varphi)) \quad (6)$$

subject to

$$\gamma_{\min} \leq \gamma \leq \gamma_{\max} \quad (7)$$

where  $\gamma_{\max}$  is computed using the following:

$$\gamma_{\max} = i, \quad \text{if} \left( \frac{p_s(0 < m \leq \varphi)}{\frac{\gamma=i+1}{p_s(0 < m \leq \varphi)} \kappa} \right) \quad \forall i, i = 1, 2, \dots \quad (8)$$

where the second term in (8) represents the effect of changing  $\gamma$  on the probability of success.  $\kappa$  is a constant used as a lower bound to prevent overextending the  $\gamma$  length beyond which its effect can be neglected. The value of  $\gamma$  is overextending when either the number of contending antennas  $vg$  and/or their transmission probability became high. In this case, the NiQ keeps increasing its SF transmission window length to achieve a higher probability of success. Overextending  $\gamma$  can result in bandwidth wastage, because the contending nodes persist for a long time to finish their SF transmission.  $\sigma\gamma$  can be found by finding the maximizer of a constrained function with one variable  $\gamma$ . Algorithm 3 lists the procedure of finding the optimal  $\sigma\gamma$ . The procedure of finding  $\sigma\gamma$  proceeds as follows: First, each node keeps track of the transmission medium activity to estimate the number of active nodes  $C_e$  and  $E[\beta]$  in each  $t_v$ . Next, it finds the  $\sigma\gamma$  value as explained in Algorithm 3. Finally, it calls lines 3–17 of Algorithm 1.

#### Algorithm 3 Finding $\sigma\gamma$

- 1: Use (8) to find  $\gamma_{\max}$ .
- 2: Set  $\gamma_{\min} = 1$ .

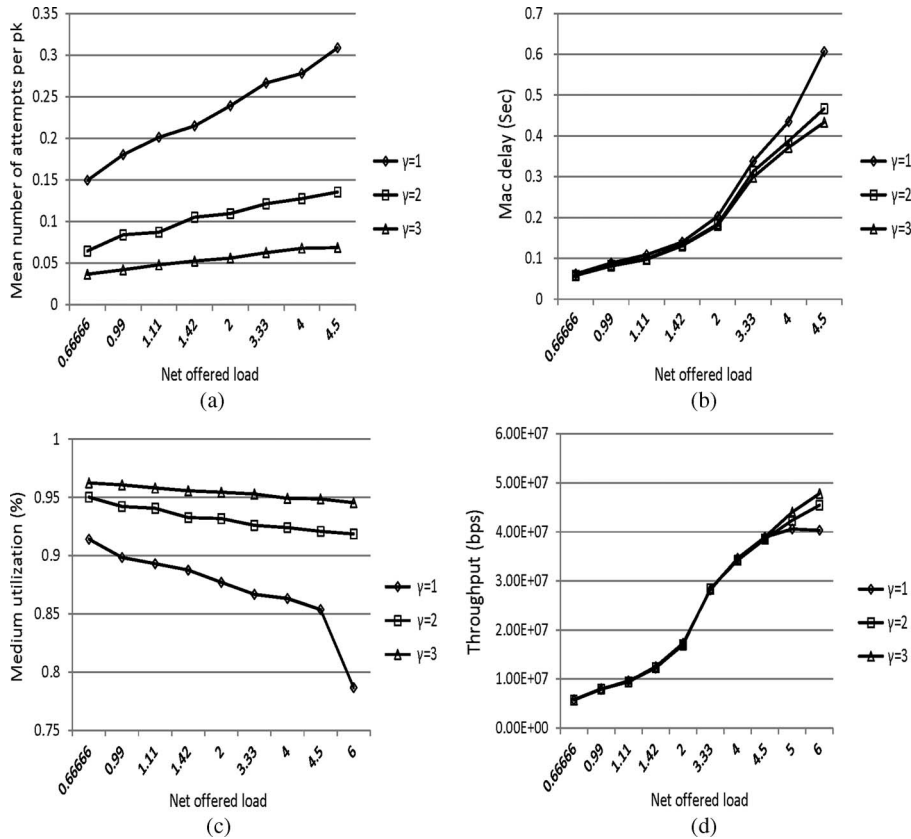


Fig. 15. Multihop network performance for different values of  $\gamma$ . (a) Mean number of attempts per packet for different  $\gamma$  lengths and network loads. (b) MAC delay for different  $\gamma$  lengths and network loads. (c) Medium utilization for different  $\gamma$  lengths and network loads. (d) Throughput for different  $\gamma$  lengths and network loads.

- 3: Find  $\gamma$  length ( $\sigma\gamma$ ) that maximizes the probability of success.
- 4: Call lines 3–17 of Algorithm 1.

To study the impact of the adaptive  $\gamma$  length on the system performance, we use the same simulation model built before. In this model, instead of assigning a fixed  $\gamma$  length for each traffic load, nodes exploit the proposed optimization program to find the  $\sigma\gamma$  length. Fig. 6 shows that using  $\sigma\gamma$  achieves a lower number of attempts per transmitted packet for all values of the used network loads. Fig. 7 shows that using  $\sigma\gamma$  length also achieves lower MAC delay, compared with using fixed  $\gamma$  lengths. Figs. 8 and 9 show that  $\sigma\gamma$  also results in higher medium utilization and throughput, respectively.

## VI. SIMULATION RESULTS: MULTIHOP NETWORK

The multihop network model is also configured with 16 stationary nodes. In this configuration, nodes are distributed apart, with distances ranging from 150 to 400 m, using the uniform distribution function in such a way that hidden nodes are formed. Due to the complexity of estimating active nodes in multihop network environments, in this work, we only evaluate the impact of exploiting the M-EDCF scheme using extensive simulation. However, if a multihop active node estimator scheme becomes available, exploiting the M-MDCF based on optimized online spatial channel sharing in multihop environments can be explored.

Because the medium access is dependent on not only its neighbors' behavior but on the behavior of hidden nodes as well, collisions in multihop networks tend to have a higher rate, compared with those in single-hop networks. The collision rate increases as the vulnerable time increases. The vulnerable time is the time interval between the medium access time of node A and the observation of node C to A's transmission if nodes A and C are out of each other's transmission ranges. Fig. 15 shows the effect of changing the SF transmission window on multiple-hop networks. Fig. 15(a) shows the mean number of attempts per packet for different  $\gamma$  lengths. Evidently, longer  $\gamma$  lengths result in a higher performance difference, compared with shorter lengths. The difference in the number of collisions for different  $\gamma$  lengths results in a MAC delay, transmission medium utilization, and throughput difference, as shown in Fig. 15(b)–(d), respectively. Note that longer  $\gamma$  lengths result in lower MAC delay, higher medium utilization, and higher throughput, compared with shorter  $\gamma$  lengths.

## VII. CONCLUSION

In this paper, we have proposed collision-mitigation enhancements to the EDCF of the IEEE 802.11e MAC protocol called the M-EDCF. The basic idea of the M-EDCF scheme is sharing the MIMO multiple spatial channels during the medium access period to avoid medium collisions. Spatial channel sharing can help transmitters to detect ongoing medium access contentions (e.g., medium attempts by other transmitters in

their vicinity); hence, they can perform early medium access termination if their SF transmission attempts cause a collision. Spatial channel sharing can help intended receivers in performing response coordinations to avoid potential collisions. We have evaluated the M-EDCF scheme over single- and multihop networks. The M-EDCF scheme results have shown fewer collisions for both networks. Activating the early contention termination and contention selection modes further reduced the number of collisions, compared with the latter at silence mode. To further improve the performance of the M-EDCF scheme, an adaptive spatial-channel-sharing scheme during the medium access period has been proposed. The proposed scheme is based on the online estimation of the number of active nodes. A node uses the estimated active node to find the optimal SF transmission window length via an optimization program that boosts the system performance in terms of reducing the number of medium access collisions and boosting the medium utilization.

Future research involves proposing a multihop active node estimation scheme and incorporating it in the M-EDCF scheme, which can adaptively reduce the effect of the hidden node problems. In addition to void collision, the M-EDCF scheme can be utilized to provide QoS differentiations during the medium-access period by controlling the SF transmission window length based on the priority class. Proposing schemes that couple the capability of collision avoidance and QoS differentiation of the M-EDCF scheme during the selection of the SF transmission window is another plan for future work.

## REFERENCES

- [1] *Part 11: Wireless LAN Medium Access Control (MAC) and Physical Layer (PHY) Specifications*, IEEE 802.11, 2007.
- [2] *Medium Access Control (MAC) Enhancements for Quality of Service (QoS)*, IEEE Amendment 8: 802.11e, Jun. 2005.
- [3] *Wireless LAN Medium Access Control (MAC) and Physical Layer (PHY) Specifications: Enhancements for Higher Throughput*, IEEE P802.11n-D4.0, Mar. 2008.
- [4] G. Bianchi, "Performance analysis of the IEEE 802.11 distributed coordination function," *IEEE J. Sel. Areas Commun.*, vol. 18, no. 3, pp. 535–547, Mar. 2000.
- [5] J. S. Kim, E. Serpedin, and D. R. Shin, "Improved particle filtering based estimation of the number of competing stations in IEEE 802.11 networks," *IEEE Signal Process. Lett.*, vol. 15, pp. 87–90, Dec. 2008.
- [6] F. Cali, M. Conti, and E. Gregori, "IEEE 802.11 protocol: Design and performance evaluation of an adaptive backoff mechanism," *IEEE J. Sel. Areas Commun.*, vol. 18, no. 9, pp. 1774–1786, Sep. 2000.
- [7] F. Cali, M. Conti, and E. Gregori, "Dynamic tuning of the IEEE 802.11 protocol to achieve a theoretical throughput limit," *IEEE/ACM Trans. Netw.*, vol. 8, no. 6, pp. 785–799, Dec. 2000.
- [8] Y. Kwon, Y. Fang, and H. Latchman, "Novel MAC protocol with fast collision resolution for wireless LANs," in *Proc. IEEE INFOCOM*, Apr. 2003, pp. 853–862.
- [9] J. Choi and J. Yoo, "EBA: An enhancement of the IEEE 802.11 DCF via distributed reservation," *IEEE Trans. Mobile Comput.*, vol. 4, no. 4, pp. 378–390, Jul./Aug. 2005.
- [10] D. Deng, C. Ke, H. Chen, and Y. Huang, "Contention window optimization for IEEE 802.11 DCF access control," *IEEE Trans. Wireless Commun.*, vol. 7, no. 12, pp. 5129–5135, Dec. 2008.
- [11] H. Kim and J. C. Hou, "Improving protocol capacity with model-based frame scheduling in IEEE 802.11-operated WLANs," *IEEE J. Sel. Areas Commun.*, vol. 22, no. 10, pp. 1987–2003, Dec. 2004.
- [12] F. Talucci, M. Gerla, and L. Fratta, "MACA-BI (MACA by invitation)—A receiver oriented access protocol for wireless multihop networks," in *Proc. IEEE Pers., Indoor, Mobile Radio Commun.*, Sep. 1997, pp. 435–439.
- [13] Z. J. Haas and J. Deng, "Dual busy tone multiple access (DBTMA)—A multiple access control scheme for ad hoc networks," *IEEE Trans. Commun.*, vol. 50, no. 6, pp. 975–985, Jun. 2002.
- [14] F. A. Tobagi and L. Kleinrock, "Packet switching in radio channels—Part III: Polling and (dynamic) split-channel reservation multiple access," *IEEE Trans. Commun.*, vol. COM-24, no. 8, pp. 832–844, Aug. 1976.
- [15] C. L. Fullmer and J. J. Garcia-Luna-Aceves, "Floor acquisition multiple access (FAMA) for packet-radio networks," in *Proc. ACM SIGCOMM*, Aug. 1995, pp. 262–273.
- [16] S. Gobriel, R. Melhem, and D. Mosse, "BLAM: An energy-aware MAC layer enhancement for wireless adhoc networks," in *Proc. IEEE Wireless Commun. Netw. Conf.*, Mar. 2005, pp. 1557–1563.
- [17] S. Romaszko and C. Blondia, "Neighbour-aware, collision avoidance MAC protocol (NCMac) for mobile ad hoc networks," in *Proc. Int. Symp. Wireless Commun. Syst.*, Sep. 2006, pp. 322–326.
- [18] H. Jin, B. C. Jung, H. Y. Hwang, and D. K. Sung, "A MIMO-based collision mitigation scheme in uplink WLANs," *IEEE Commun. Lett.*, vol. 12, no. 6, pp. 417–419, Jun. 2008.
- [19] S. A. Jafar and M. J. Fakhreddin, "Degrees of freedom for the MIMO interference channel," *IEEE Trans. Inf. Theory*, vol. 53, no. 7, pp. 2637–2642, Jul. 2007.
- [20] D. Tse and P. Viswanath, *Fundamentals of Wireless Communication*. Cambridge, U.K.: Cambridge Univ. Press, 2005.
- [21] D. C. Montgomery and G. C. Runger, *Applied Statistics and Probability for Engineers*, 3rd ed. Hoboken, NJ: Wiley, 2003.



**Abduladhim Ashtaiwi** (A'09) received the B.Sc. degree in electrical and electronic engineering from Bright Star University of Technology, Brega Hereby, Libya, in 1992 and the M.Sc. and Ph.D. degrees from Queen's University, Kingston, ON, Canada, in 2004 and 2009, respectively.

He is currently a Research Associate with the Department of Electrical and Computer Engineering, Queen's University. He has authored several publications, including journal papers, refereed conference proceeding papers, and book chapters. His research interests include fourth-generation-and-beyond wireless network architectures, wireless local area network protocols and standards, cross-layer design and optimization, multiple-input-multiple-output systems, wireless ad hoc and sensor networks, radio resource management, wireless medium access control techniques, quality-of-service routing, and resource reservation.



**Hossam Hassanein** (S'85–M'90–SM'05) received the Ph.D. degree in computing science from the University of Alberta, Edmonton, AB, Canada, in 1990.

He is currently with the School of Computing, Queen's University, Kingston, ON, Canada, working in the areas of broadband, wireless and variable topology network architectures, protocols, and control and performance evaluation. He is the Founder and Director of the Telecommunication Research Laboratory (<http://www.cs.queensu.ca/~trl>), School

of Computing, Queen's University. He has more than 350 publications in reputable journals, conference proceedings, and workshops in the areas of computer networks and performance evaluation.

Dr. Hassanein has organized and served on the program committees of numerous international conferences and workshops. He is currently the Vice-Chair of the IEEE Communication Society Technical Committee on Ad hoc and Sensor Networks. He also serves on the editorial boards of a number of international journals. He is an IEEE Communications Society Distinguished Lecturer. He has delivered several invited talks and tutorials at key international venues, including Unconventional Computing 2007, IEEE ICC 2008, IEEE WLN 2008, IEEE CCNC 2009, IEEE GCC 2009, and IEEE GIIS 2009. He was the recipient of the Communications and Information Technology Ontario Champions of Innovation Research Award in 2003 and the Best Paper Awards at the IEEE Wireless Communications and Networks and the IEEE Global Communication Conferences (both flagship IEEE Communications Society conferences) in 2007.